Available online at www.sciencedirect.com
ScienceDirect
Journal of Sound and Vibration 322 (2009) 155–166
JOURNAL OF SOUND AND VIBRATION
www.elsevier.com/locate/jsvi

Experimental statistical energy analysis of coupled plates with wave conversion at the junction

C. Hopkins*

Acoustics Research Unit, School of Architecture, University of Liverpool, Liverpool L69 7ZN, UK

Received 27 March 2008; received in revised form 25 September 2008; accepted 29 October 2008
Handling Editor: C.L. Morfey
Available online 12 December 2008

Abstract

Coupling loss factors for bending wave transmission between coupled plates can be determined using experimental statistical energy analysis. However, some types of plate junctions introduce significant wave conversion such that the assumption of a statistical energy analysis (SEA) system that supports only bending waves is no longer appropriate. Three methods have been assessed to identify the existence of wave conversion between bending and in-plane waves when experimental SEA is used to analyse a system that is assumed to consist of only bending wave subsystems. These methods were based on errors in the internal loss factor, matrix condition numbers, and a failure to satisfy the consistency relationship. Only the former method that calculated errors in the predicted internal loss factors was found to be of use in identifying wave conversion.

1. Introduction

Analysis of bending wave transmission in engineering structures over the audio frequency range is often carried out by subdividing a structure into beam and plate subsystems that can be modelled using statistical energy analysis (SEA) [1]. The subsystems are coupled together at junctions where the type of connection may be sufficiently straightforward that theoretical models can be used. However, the connection can be sufficiently complicated that a validated model is not available, or sufficiently accurate. In such situations it is common to determine the coupling loss factors (CLFs) by using measurements of bending wave vibration in the laboratory or *in-situ*. Alternatively, the CLFs can be determined from numerical models. Finite element methods (FEM) have proven to be a practical way of generating such input data e.g. [2–6]. For a small number of plates coupled together at a junction, experimental SEA (ESEA) essentially treats the junction as a 'black box' upon which there is an incident bending wave field on the source plate that results in a transmitted bending wave field on the receiving plate. The process of wave conversion is hidden within this 'black box'. Hence in the absence of a model for the junction, a common and convenient assumption is that wave conversion from bending into in-plane waves can be ignored, or does not take place. This situation is

*Tel.: +44 151 794 4938.
E-mail address: carl.hopkins@liv.ac.uk

0022-460X/$ - see front matter © 2008 Elsevier Ltd. All rights reserved.
doi:10.1016/j.jsv.2008.10.025

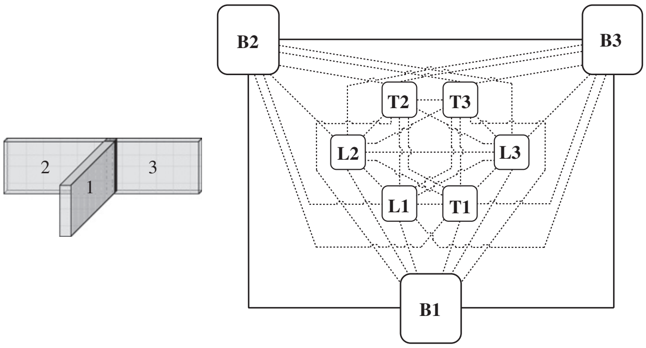

Fig. 1. *T*-junction of coupled plates (the black box at the junction indicates an unspecified type of connection between the plates) and the associated SEA model. SEA subsystems are shown for bending (B), quasi-longitudinal (L) and transverse shear (T) waves. In experimental forms of SEA it is common to consider only the bending wave subsystems; hence all the coupling to in-plane wave subsystems indicated by the dotted lines is effectively ignored.

illustrated in Fig. 1 with an example SEA model for three coupled plates that form a *T*-junction. Considering this example it is evident that such assumptions run the risk of significantly oversimplifying the 'true' model so that errors will occur when the experimental CLFs are included in an SEA model of the full structure. Another problem is that the experimental CLFs may not be situation-invariant, i.e. the coupled plates tested with ESEA will perform significantly differently *in-situ* because no account is taken of different damping for the in-plane wave subsystems.

Experimental forms of SEA are relevant to the building, marine, automotive and aeronautic industries. For building constructions, SEA models validated with measurements have confirmed the importance of in-plane waves in the transmission of vibration between coupled plates made of concrete and masonry [7]. This in-plane wave transmission becomes particularly important when predicting transmission between non-adjacent rooms [8]. However, it has been found that measurement of in-plane energy above 500 Hz is highly prone to error due to thick plate effects and the coexistence of bending wave motion [9]. For marine structures such as ships, the importance of in-plane motion has also been noted when the transmission path involves several interconnected plates [10]. Early work on the experimental determination of CLFs focussed on thin metal plates for which experimental errors and matrix inversion problems were the main issue because in-plane wave transmission was not an important transmission mechanism [11,12]. In reviewing automotive applications of ESEA with laboratory measurements, Cimerman et al. [13] noted the limitation that only bending wave transmission could be quantified between coupled subsystems. This was because of the difficulty in accurately measuring in-plane wave motion in the presence of bending vibration. However, no solution was proposed to identify or account for significant effects of wave conversion.

This paper assesses methods of identifying wave conversion in ESEA without recourse to inaccurate and awkward measurements of in-plane wave vibration in the presence of bending wave motion. The plate junction that is used as an example is based on heavyweight building constructions where the plates are made from concrete or masonry, although it should be noted that wave conversion is also important with ribbed plates such as timber joist floors in lightweight buildings. Laboratory measurements that can quantify vibration transmission between connected wall/floor elements are particularly useful for complicated junctions such as those involving resilient materials, point connections, foundations, steps or staggers. This application is also of interest because in building acoustics there is a well-defined frequency range of interest that is specified in third-octave bands between 50 and 5 kHz. Between 50 and 500 Hz, concrete/masonry plates tend to act as thin plates with low mode counts and low modal overlap for bending wave motion. Above 500 Hz the plates begin to support in-plane modes, hence just as the plate subsystems begin to support large numbers of bending modes, it becomes necessary to consider the existence of transverse shear and quasi-longitudinal wave subsystems which have low mode counts [14]. This paper extends previous work by Hopkins [5] that investigated the use of ESEA with FEM for coupled plate systems with low modal density and low modal overlap. These systems supported only bending wave motion and the focus was only on the low-frequency range. This paper extends the analysis to consider the effects of wave conversion to in-plane waves in the mid- and high-frequency range.

2. ESEA-techniques

The general equations from SEA can be rearranged to give a number of different matrix formulations for ESEA. The general ESEA formulation is given as follows:

$$\begin{bmatrix} \sum_{n=1}^{N}\eta_{1n} & -\eta_{21} & \cdots & -\eta_{N1} \\ -\eta_{12} & \sum_{n=1}^{N}\eta_{2n} & & \\ \vdots & & \ddots & \\ -\eta_{1n} & & & \sum_{n=1}^{N}\eta_{Nn} \end{bmatrix} \begin{bmatrix} E_{11} & E_{12} & \cdots & E_{1N} \\ E_{21} & E_{22} & & \\ \vdots & & \ddots & \\ E_{N1} & & & E_{NN} \end{bmatrix} = \begin{bmatrix} \Pi_{\mathrm{in},1}/\omega & 0 & \cdots & 0 \\ 0 & \Pi_{\mathrm{in},2}/\omega & & 0 \\ \vdots & & \ddots & \\ 0 & 0 & \cdots & \Pi_{\mathrm{in},N}/\omega \end{bmatrix} \tag{1}$$

where η_{ii} is the internal loss factor (ILF) of subsystem i, η_{ij} is the CLF from subsystem i to j, E_{ij} is the energy of subsystem i with power input into subsystem j, and $\Pi_{\mathrm{in},j}$ is the power input to subsystem j.

If the energy matrix is ill-conditioned the accuracy of its inverse can depend upon the matrix inversion; for these calculations the matrix inversions are carried out using LU decomposition, Crout's method with partial pivoting.

Previous work [5] on different matrix formulations concluded that the general ESEA formulation in Eq. (1) typically gave the lowest condition numbers and can be considered as a robust formulation. However, an alternative ESEA formulation from Lalor [15] can sometimes give slightly lower condition numbers than the general formulation and avoid ill-conditioned matrices that sometimes occur. The alternative ESEA formulation determines the CLFs and the ILFs separately; this is done by solving the following matrix equations:

$$\begin{bmatrix} \eta_{1i} \\ \vdots \\ \eta_{ri} \\ \vdots \\ \eta_{Ni} \end{bmatrix}_{r\neq i} = \frac{\Pi_{\mathrm{in},i}}{\omega E_{ii}} \begin{bmatrix} \left(\frac{E_{11}}{E_{i1}}-\frac{E_{1i}}{E_{ii}}\right) & \cdots & \left(\frac{E_{r1}}{E_{i1}}-\frac{E_{ri}}{E_{ii}}\right) & \cdots & \left(\frac{E_{N1}}{E_{i1}}-\frac{E_{Ni}}{E_{ii}}\right) \\ \vdots & \ddots & & & \vdots \\ \vdots & & \left(\frac{E_{rr}}{E_{ir}}-\frac{E_{ri}}{E_{ii}}\right) & & \vdots \\ \vdots & & & \ddots & \vdots \\ \left(\frac{E_{1N}}{E_{iN}}-\frac{E_{1i}}{E_{ii}}\right) & \cdots & \left(\frac{E_{rN}}{E_{iN}}-\frac{E_{ri}}{E_{ii}}\right) & \cdots & \left(\frac{E_{NN}}{E_{iN}}-\frac{E_{Ni}}{E_{ii}}\right) \end{bmatrix}^{-1} \begin{bmatrix} 1 \\ \vdots \\ \vdots \\ \vdots \\ 1 \end{bmatrix} \tag{2}$$

$$\begin{bmatrix} \eta_{11} \\ \vdots \\ \eta_{NN} \end{bmatrix} = \frac{1}{\omega} \begin{bmatrix} E_{11} & \cdots & E_{N1} \\ \vdots & \ddots & \vdots \\ E_{1N} & \cdots & E_{NN} \end{bmatrix}^{-1} \begin{bmatrix} \Pi_{\mathrm{in},1} \\ \vdots \\ \Pi_{\mathrm{in},N} \end{bmatrix} \tag{3}$$

With both the general and alternative ESEA formulations, the choice and number of subsystems under consideration, as well as errors in the energies will sometimes result in negative loss factors. These have no physical meaning hence it is necessary to reassess the choice of subsystems and consider the uncertainty in the energies. The latter can be accounted for by considering the confidence intervals for the mean energies from measurements or numerical models. However, with numerical models there is the possibility of creating an ensemble of similar subsystems based on the uncertainty that exists in describing subsystem properties such as mass, dimensions, stiffness, damping etc. [5]. This is beneficial in identifying systems where the problem of negative loss factors only occur with a few members of the ensemble.

For the general and alternative ESEA formulations it is noted that if the system is modelled with ESEA assuming only bending subsystems, then no account is taken of energy stored within the in-plane subsystems. Although this violates the conservation of energy, the matrix inversion may still produce a unique solution, albeit it a solution for which the derived loss factors describe a different system to the one under investigation. This issue is clearly important when ESEA is used to quantify CLFs for complicated junction connections.

ESEA measurements of vibration transmission on real building structures do not always allow measurement of the power input because of the difficulty in fixing force transducers and impedance heads. A simpler version of ESEA that avoids errors with matrix inversion is to assume that in the system under study, the source and receiver subsystem of interest form a two-subsystem SEA model. This requires the total loss factor of the receiver subsystem to be sufficiently high that equipartition of modal energy does not occur. It also requires any of the other connected subsystems to act as places of energy dissipation, not as conduits for flanking transmission between the source and receiver subsystems. This allows each CLF to be calculated using

$$\eta_{ij} = \frac{E_j}{E_i}\eta_j \tag{4}$$

where E_i is the energy of source subsystem i, E_j is the energy of receiver subsystem j, and η_j is the total loss factor of subsystem j.

Compared with the matrix formulations, this simple approach does not produce negative loss factors. Whilst this may seem advantageous, the approach is problematic in the sense that it is difficult to judge whether the choice of the two subsystems is appropriate, and whether significant wave conversion has taken place.

3. Example system of coupled plates

In order to assess methods of identifying wave conversion, an example system of coupled plates is chosen that applies to heavyweight building structures (e.g. concrete, masonry). With buildings the walls and floors are typically connected at right angles to each other and the most common types of junction are *L*-, *T*-, and *X*-junctions for two, three and four plates, respectively. For heavyweight walls and floors with rigid connections at the junction, the effect of wave conversion tends to be more significant with *T*- and *X*-junctions. For this reason, the coupled plate system used as an example in this paper is a *T*-junction of three plates as indicated in Fig. 1.

The dimensions for plates 1, 2 and 3 are $x_1 = 4\,\mathrm{m}$, $x_2 = 3.5\,\mathrm{m}$, $x_3 = 3\,\mathrm{m}$, $y_1 = y_2 = y_3 = 2.4\,\mathrm{m}$ with the plates connected along the y-dimension. The plate thicknesses are $h_1 = 0.215\,\mathrm{m}$, $h_2 = h_3 = 0.1\,\mathrm{m}$. The densities are $\rho_1 = 2000\,\mathrm{kg/m^3}$, $\rho_2 = \rho_3 = 600\,\mathrm{kg/m^3}$. The longitudinal wavespeeds are $c_{L1} = 3200\,\mathrm{m/s}$, $c_{L2} = c_{L3} = 1900\,\mathrm{m/s}$. The Poisson ratios are: $v_1 = v_2 = v_3 = 0.2$. The plates are rigidly bonded together at the junction as they would be with interleaved masonry or poured concrete. To simulate total loss factors representative of fully connected walls in complete buildings, the frequency-dependent ILF in the FEM model was specified as $1/\sqrt{f}$ where f is the band centre frequency. Such highly damped systems are advantageous for ESEA because there are relatively few problems with negative loss factors resulting from the matrix inversion. The lowest third-octave bands in which the fundamental local mode lies for bending (B), transverse shear (T) and quasi-longitudinal (L) are 80 Hz (B), 500 Hz (T) and 800 Hz (L) for plate 1, and 25 Hz (B), 315 Hz (T) and 500 Hz (L) for plates 2 and 3.

The *T*-junction was modelled using both SEA and FEM. The SEA models used wave theory to calculate the transmission coefficients for bending waves only, and for bending, quasi-longitudinal and transverse shear waves [14]. The FEM calculations were carried out using ANSYS software with SHELL63 elements and element dimensions smaller than one-sixth of the bending wavelength. Comparisons of FEM, SEA and measurements have previously been made on a *T*-junction of full-size masonry walls that were rigidly bonded together [16]. These confirm that the FEM model is valid and that in-plane wave transmission occurs at high frequencies. In addition they show that the element nodes along the junction line must be unconstrained in order to correctly describe transmission across the straight section of the *T*-junction. For the numerical experiments in this paper the FEM models used a simply supported junction line to ensure only bending wave transmission across the junction, and an unconstrained junction line to allow bending and in-plane wave transmission across the junction.

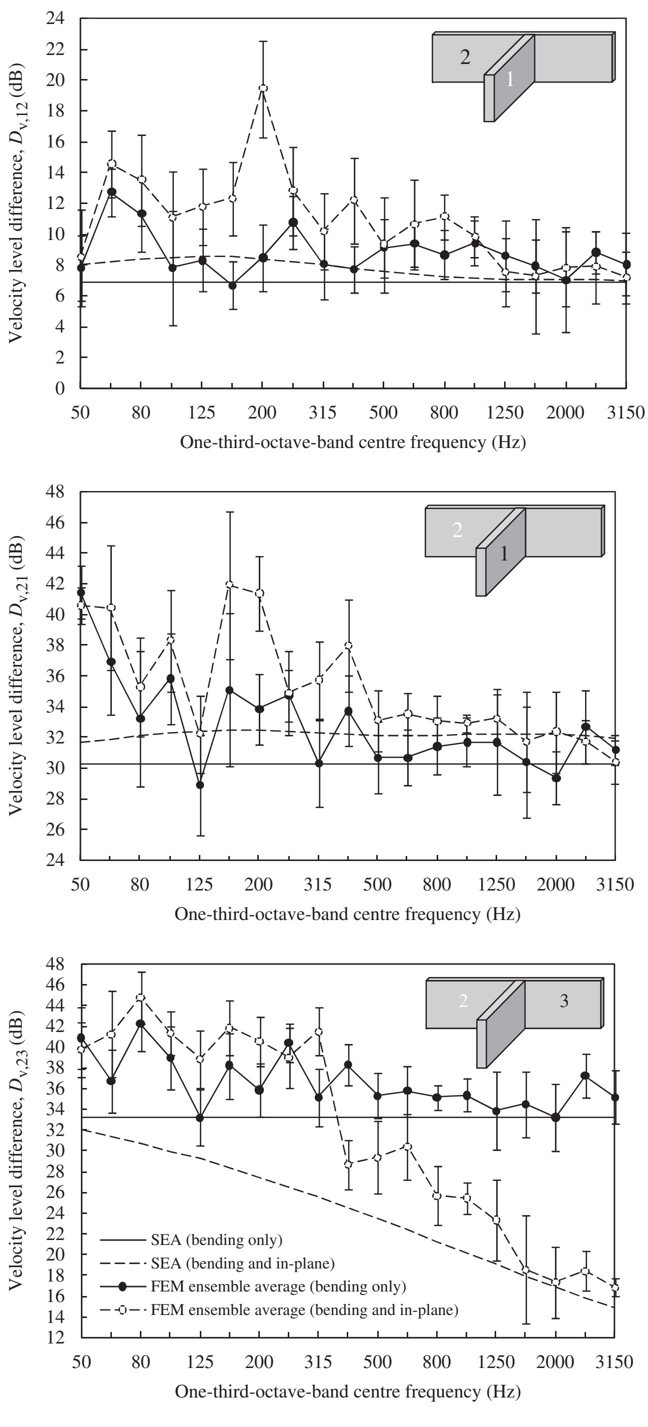

Fig. 2. Velocity level differences, $D_{v,ij}$, between bending wave subsystems where *i* is the source subsystem and *j* is the receiving subsystem. The FEM ensemble is represented by its mean value with 95% confidence intervals.

For plates with relatively low modal densities it is rarely appropriate to draw conclusions based on a single deterministic analysis with FEM; hence an ensemble of *T*-junctions was created and ESEA analysis was carried out on each member of the FEM ensemble. The ensemble was created through the use of random numbers drawn from a normal distribution, $N(\mu,\sigma)$, to vary the wall length perpendicular to the junction for

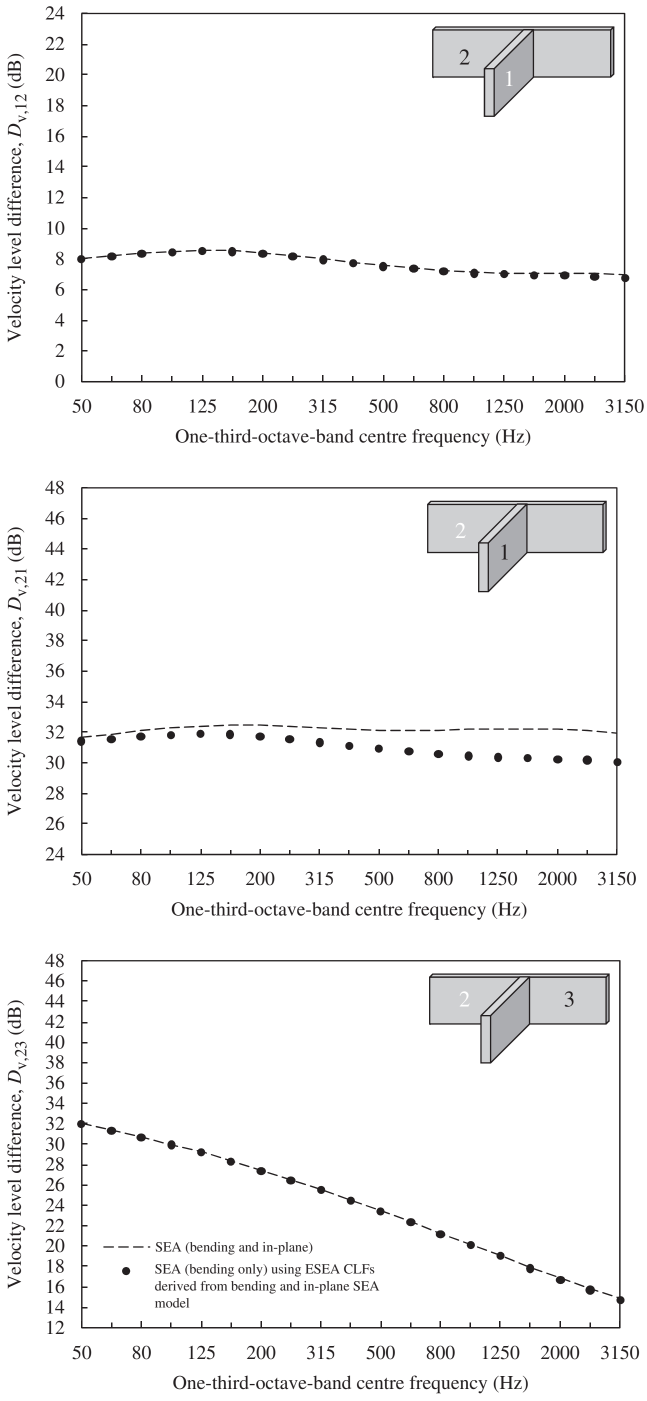

Fig. 3. Velocity level differences, $D_{v,ij}$, for the comparison of the full SEA model for bending and in-plane wave subsystems with the three bending subsystem SEA model using coupling loss factors derived using ESEA with the output from the full SEA model.

all three plates. This used the plate x-dimension as the mean value, μ, with a standard deviation, $\sigma = 0.25$ m. Due to time constraints on computation, the FEM ensemble contained ten members for third-octave bands between 50 Hz and 1 kHz, and five members between 1.25 and 3.15 kHz.

3.1. Effects of wave conversion

Fig. 2 shows the velocity level difference, $D_{v,ij}$, between source (i) and receiving (j) bending wave subsystems with excitation of bending waves on the source subsystem. Both SEA and FEM show a similar variation with frequency. However, these plates have relatively low modal density and modal overlap. This results in the large fluctuations shown by the FEM model, and discrepancies between FEM and SEA. Wave conversion at the junction has a particularly pronounced effect on vibration transmission across the straight section of the T-junction ($D_{v,23}$) at frequencies above the fundamental transverse shear and quasi-longitudinal local modes of the three plates. An assessment can now be made to see what happens when the SEA system consisting of nine subsystems is subsequently modelled as an ESEA system comprising only three bending wave subsystems. The CLFs determined from ESEA between bending wave subsystems can then be used to create a new SEA model using only three subsystems. A comparison between the original SEA model for bending and in-plane wave subsystems can be compared with this three bending subsystem SEA model in Fig. 3. This illustrates the deceptive nature of ESEA in that the predictions of $D_{v,12}$ and $D_{v,23}$ give the impression that the bending only model adequately describes the transmission process. The only indication that the model may be inappropriate occurs with $D_{v,21}$ at high frequencies where there is a discrepancy between the two predictions. In this example the errors for the isolated T-junction can be considered negligible, and will only become significant once the T-junction is incorporated as part of a larger system involving many more subsystems, and predictions are made for vibration transmission across more than one junction.

4. Potential methods to identify wave conversion

This section assesses different methods of identifying wave conversion when using ESEA to model each plate as a bending wave subsystem and no attempt is made to measure in-plane wave motion.

4.1. The effect of wave conversion on errors in the ILF

Values for the ILF of each subsystem are usually determined from measurements on isolated test specimens. However, the ESEA matrix inversion also produces these values; hence a check can be made against the specified ILF in the numerical model or the expected ILF in the physical experiment. The error, $e(\eta_{ii})$, in decibels for each subsystem i can be defined using

$$e(\eta_{ii}) = 10\,\mathrm{lg}\left(\frac{\eta_{ii(\mathrm{ESEA})}}{\eta_{ii}}\right) \tag{5}$$

where η_{ii} is the actual ILF and $\eta_{ii(\mathrm{ESEA})}$ is the ILF determined from ESEA.

This definition means that $e(\eta_{ii})$ is undefined for zero or negative $\eta_{ii(\mathrm{ESEA})}$ for which the matrix inversion can be considered to have failed and ESEA 'weak' coupling does not occur. When $\eta_{ii(\mathrm{ESEA})}$ has a finite positive value, $e(\eta_{ii})$ can be either positive or negative from which it may be inferred that ESEA 'weak' coupling occurs. Values of 0 dB for $e(\eta_{ii})$ occur when there is exact agreement between the actual ILF and the ILF derived from ESEA.

SEA models with only bending wave theory, and with bending and in-plane wave theory were used to generate input data for ESEA. The resulting ESEA ILF errors are shown in Fig. 4a; and as would be expected, there is no error (0 dB) for the SEA model with only bending waves. The ESEA ILF errors using the FEM ensemble are shown in Fig. 4b. For this T-junction, the ESEA ILF errors are the same for both the general and the alternative ESEA formulation; hence the values in the figures correspond to either formulation. Above 200 Hz, the trend indicated by the SEA model (bending and in-plane) is also seen with the FEM ensemble; namely, that the ESEA ILF error increases with increasing frequency for plate 1 at frequencies above the fundamental transverse shear and quasi-longitudinal local modes of the three plates. The reason for this is that

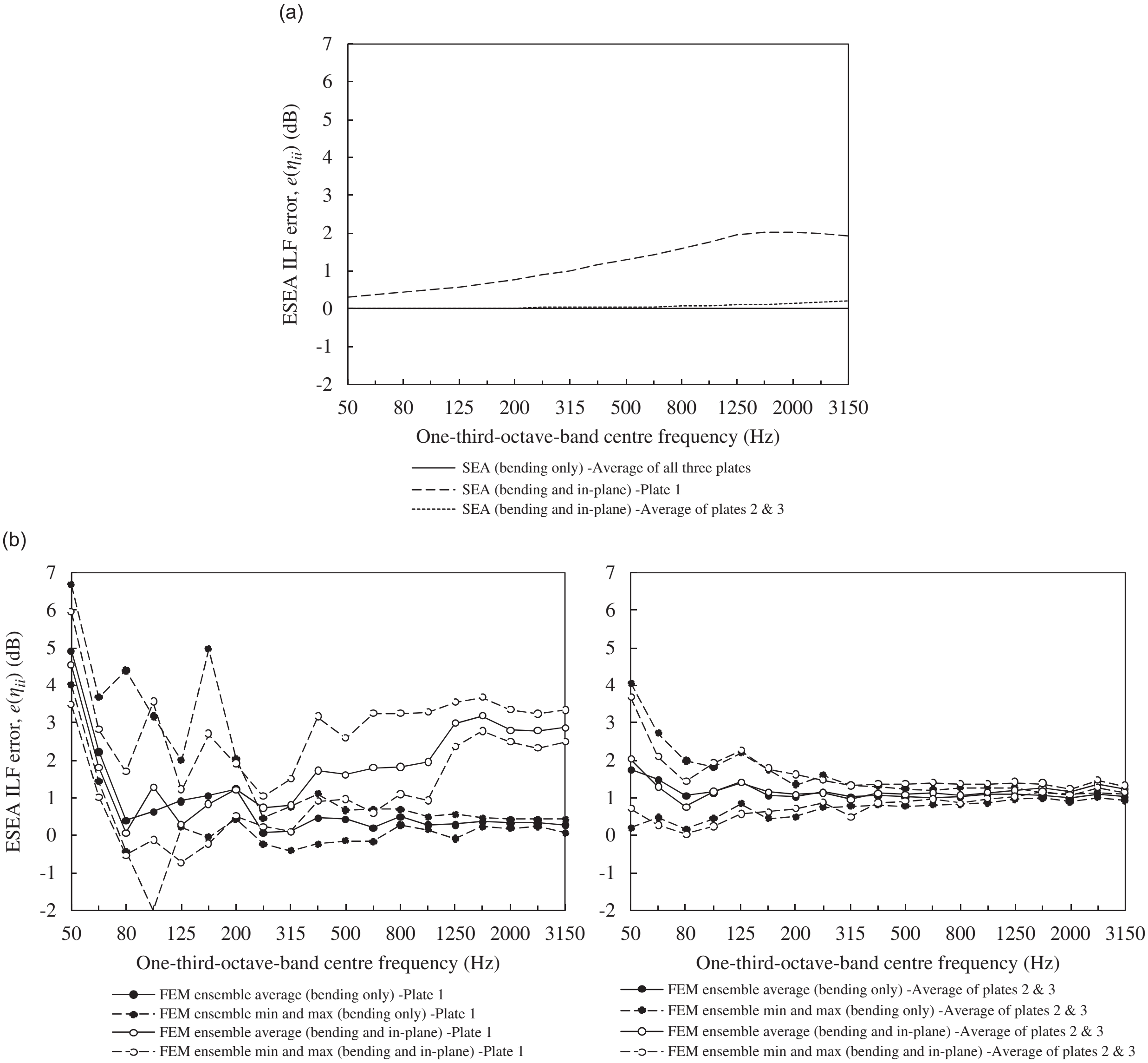

Fig. 4. Errors in the internal loss factor derived using ESEA: (a) SEA model and (b) FEM ensemble.

by assuming only three bending subsystems, the in-plane subsystems are merely considered as places of energy dissipation, rather than part of the transmission path. Hence a bending wave ESEA model will overestimate the actual ILF for some of the plate bending subsystems. The fact that the ESEA ILF error is sometimes only significant for one plate in a T-junction indicates the importance in checking the ESEA ILF error of all subsystems. This is clearly essential if wave conversion is to be identified when using ESEA with plate junctions for which there is no valid prediction model.

Apart from rigidly connected T- and X-junctions in buildings, the effects of wave conversion can be significant when resilient materials are introduced at the junction of heavyweight walls and floors. To check whether the ESEA ILF error could identify wave conversion for these resilient junctions, SEA models of different junctions have been created using wave theory [17] to calculate transmission coefficients for bending, quasi-longitudinal and transverse shear waves. In most cases the errors above the fundamental transverse shear and quasi-longitudinal local modes were very similar to the example shown in this paper for the rigidly connected T-junction. However, there are a large number of permutations for the position/alignment and dynamic properties of the resilient material at the junction, as well as for the plate properties. Permutations were occasionally found for which the error was insignificant; hence the ESEA ILF error will not always identify the process of wave conversion.

4.2. The effect of wave conversion on the matrix condition number

For systems of coupled plates with low modal density and low modal overlap the condition number for the matrix inversion can be quite high [5,18]. The intention is to see whether there is a detectable change in the condition number when a coupled system that is represented only by bending subsystems is changed from supporting only bending waves, to both bending and in-plane waves.

The general or alternative ESEA formulations both require inversion of an energy matrix, **E**, to determine the loss factors. The condition number of the energy matrix, $\kappa(\mathbf{E})$, measures the sensitivity of $\mathbf{E}^{-1}$ to small changes in the matrix entries of **E**. For ideal square matrices, the condition number is unity and the matrix problem is well-conditioned. When the condition number is much larger than unity, the matrix problem is ill-conditioned such that small errors in the individual energies can cause large errors in the calculated loss factors. The condition number has been calculated using the Euclidean norm (sometimes called the L_2-norm) which is the square root of the sum of the squares of the matrix elements. Different norms exist which therefore results in different condition numbers, hence it is not the absolute values that are of interest, but rather the change in condition number when a system begins to support in-plane wave motion as well as bending wave motion.

The matrix condition numbers are shown in Fig. 5. The lowest condition numbers tend to occur with the SEA models that only consider bending wave vibration. This is expected because the matrix is quite well-conditioned due to an identical number of subsystems in both the SEA and ESEA models. However, the SEA model for bending and in-plane waves has similar condition numbers to the SEA model for bending waves, with only a slight increase due to the existence of in-plane waves. A larger increase might have been expected because a three subsystem ESEA model has been used with data from a nine subsystem SEA model. However this finding is specific to this particular system of coupled plates and larger increases can be expected with other systems. More importantly, the relatively high condition numbers from the FEM models indicate that the condition number is not a useful indicator of wave conversion because (a) there are significant differences between the general and alternative matrix formulations and (b) low condition numbers sometimes occur when there is significant in-plane energy that is ignored with ESEA that only considers bending subsystems. For the general ESEA matrix formulation with the FEM ensemble in Fig. 5b, it is reasonable to consider the possibility that the increased range for the condition number at 800 Hz is due to the local fundamental quasi-longitudinal mode supported by plate 1. However, experiments with other L- and T-junctions indicate that significant changes in the condition number do not always occur at the cut-on frequency for local in-plane modes [19].

4.3. The effect of wave conversion on checks using the consistency relationship

Lalor [15] noted that for three subsystems connected in a closed loop, it is possible to use the consistency relationship to check the quality of the CLFs determined using ESEA. Assuming equipartition of modal energy in subsystems i and j, the SEA consistency relationship is given by

$$\frac{\eta_{ij}}{n_j} = \frac{\eta_{ji}}{n_i} \tag{6}$$

where n is the modal density.

Hence for three subsystems that are all connected to each other, there are three consistency relationships that need to be satisfied and these can be combined to give the following relationship:

$$\frac{\eta_{ij}\eta_{jk}\eta_{ki}}{\eta_{ji}\eta_{ik}\eta_{kj}} = 1 \tag{7}$$

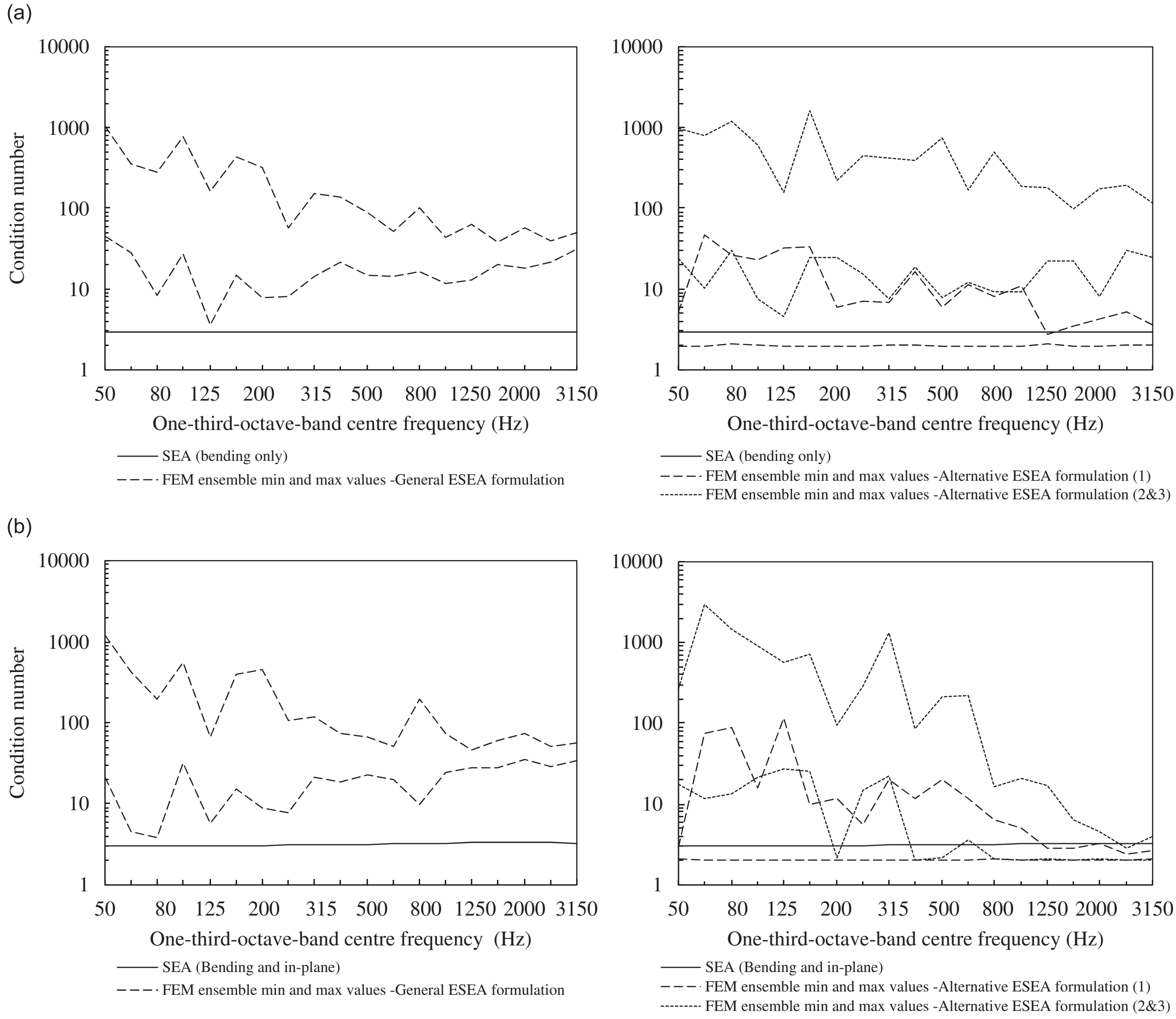

Fig. 5. Matrix condition numbers from the general and alternative ESEA formulations for an ESEA system comprising three bending subsystems. Note that the alternative ESEA formulation is used to determine the CLFs to a subsystem hence, (1) in the legend corresponds to the matrix inversion used to determine η_{21} and η_{31}, and (2 and 3) in the legend corresponds to the matrix inversions used to determine η_{12}, η_{32}, η_{13} and η_{23}: (a) SEA and FEM ensemble where only bending waves are generated at the junction and (b) SEA and FEM ensemble where bending and in-plane waves are generated at the junction.

This applies to *i*, *j* and *k* as bending subsystems, or transverse shear subsystems, or quasi-longitudinal subsystems, but not combinations of the different wave types. For this reason, this relationship is only likely to indicate wave conversion if significant errors are introduced through the matrix inversion.

The CLF ratio on the left-hand side of Eq. (7) can be compared with a value of unity on Fig. 6 for the general ESEA formulation; note that the values for the alternative ESEA formulation are nominally the same. There is a relatively wide spread of values and as the ratio does not converge to unity for the FEM ensemble (bending only) it is not a useful indicator of wave conversion.

The CLF ratio from measurements using Eq. (4) on two full-size *T*-junctions of masonry walls (construction details given in Refs. [14,16]) are shown in Fig. 7. These data are more tightly clustered around unity and give no indication that wave conversion is occurring above 500 Hz.

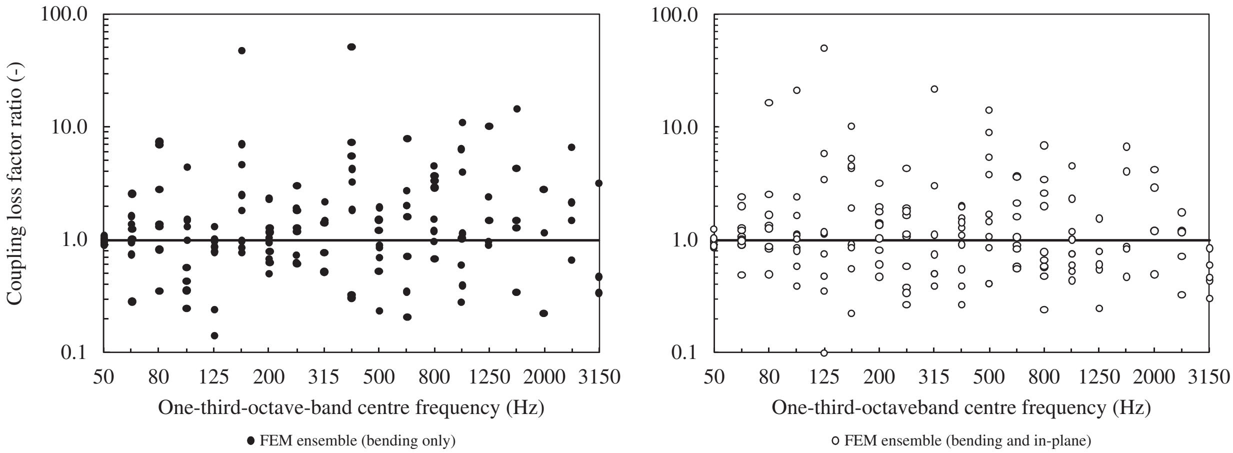

Fig. 6. Coupling loss factor ratio (Eq. (7)) for three bending wave subsystems connected in a closed loop using coupling loss factors derived from the FEM ensemble with ESEA.

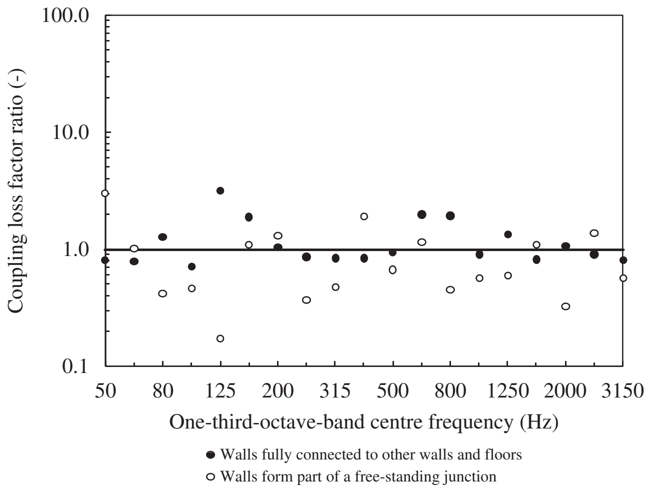

Fig. 7. Coupling loss factor ratio (Eq. (7)) from measurements on two *T*-junctions formed from masonry walls.

5. Conclusions

ESEA using physical measurements or numerical models is a highly useful tool for quantifying vibration transmission between plates that are connected at complicated junctions. However, treating the junction as a black box and assuming only bending waves are transmitted at the junction can result in unrepresentative SEA models if there is significant wave conversion into in-plane wave energy. Three methods have been assessed to try and identify wave conversion between bending and in-plane waves when ESEA is used to analyse a system that is assumed to consist of only bending wave subsystems. These methods were based on errors in the ILF, matrix condition numbers, and a failure to satisfy consistency relationships. The construction used to test these methods was based on a *T*-junction of heavyweight walls in a building. For such plate subsystems where the modal overlap and mode counts are relatively low for bending and in-plane modes, methods based on matrix condition numbers and the consistency relationship were of little or no use in identifying wave conversion. A more useful approach was to calculate and assess the errors in the predicted ILF. The internal losses are usually known *a priori* and tend to be frequency-independent; this simplifies the identification of errors due to wave conversion. However, significant errors will not always occur in the ILF of every subsystem that is connected to the junction; for this reason the errors need to be checked in all the subsystems. In testing this approach with junctions that incorporated resilient materials, it was found that there would occasionally be permutations of plate and resilient material for which there were no significant errors in the predicted ILF, even though significant wave conversion took place. This serves to emphasize the degree of caution that is needed with ESEA and the importance of developing junction transmission models for complicated junctions that can be incorporated in predictive SEA.

References

[1] R.H. Lyon, R.G. DeJong, *Theory and Application of Statistical Energy Analysis*, second ed., Butterworth-Heinemann, 1995.
[2] C. Simmons, Structure-borne sound transmission through plate junctions and estimates of SEA coupling loss factors using the finite element method, *Journal of Sound and Vibration* 144 (1991) 215–227.
[3] J.A. Steel, R.J.M. Craik, Statistical energy analysis of structure-borne sound transmission by finite element methods, *Journal of Sound and Vibration* 178 (1994) 553–561.
[4] C.R. Fredo, A SEA-like approach for the derivation of energy flow coefficients with a finite element model, *Journal of Sound and Vibration* 199 (1997) 645–666.
[5] C. Hopkins, Statistical energy analysis of coupled plate systems with low modal density and low modal overlap, *Journal of Sound and Vibration* 251 (2) (2002) 193–214.
[6] A.N. Thite, B.R. Mace, Robust estimation of coupling loss factors from finite element analysis, *Journal of Sound and Vibration* 303 (2007) 814–831.
[7] T. Kihlman, Transmission of structure-borne sound in buildings, Report 9/67, National Swedish Institute for Building Research, 1967.
[8] R.J.M. Craik, A. Thancanamootoo, The importance of in-plane waves in sound transmission through buildings, *Applied Acoustics* 37 (1992) 85–109.
[9] R.J.M. Craik, In-plane wave propagation in buildings, *Applied Acoustics* 53 (4) (1998) 273–289.
[10] R.H. Lyon, In-plane contribution to structural noise transmission, *Noise Control Engineering Journal* 26 (1) (1986) 22–27.
[11] D.A. Bies, S. Hamid, *In situ* determination of loss and coupling loss factors by the power injection method, *Journal of Sound and Vibration* 70 (2) (1980) 187–204.
[12] B.L. Clarkson, M.F. Ranky, On the measurement of the coupling loss factor of structural connections, *Journal of Sound and Vibration* 94 (2) (1984) 249–261.
[13] B. Cimerman, T. Bharj, G. Borello, Overview of the experimental approach to Statistical Energy Analysis, *Proceedings of the Society of Automotive Engineers—Noise and Vibration Conference*, Paper 971968, 1997.
[14] C. Hopkins, *Sound Insulation*, Butterworth-Heinemann, Imprint of Elsevier, Oxford, 2007 ISBN: 978-0-7506-6526-1.
[15] N. Lalor, Practical considerations for the measurement of internal and coupling loss factors on complex structures, ISVR Technical Report No. 182, June 1990.
[16] C. Hopkins, Vibration transmission between coupled plates using finite element methods and statistical energy analysis. Part 1: comparison of measured and predicted data for masonry walls with and without apertures, *Applied Acoustics* 64 (10) (2003) 955–973.
[17] P. Mees, G. Vermeir, Structure-borne sound transmission at elastically connected plates, *Journal of Sound and Vibration* 166 (1) (1993) 55–76.
[18] M. Heckl, M. Lewit, Statistical energy analysis as a tool for quantifying sound and vibration transmission paths, *Philosophical Transactions of the Royal Society of London A* 346 (1994) 449–464.
[19] C. Hopkins, Structure-borne Sound Transmission Between Coupled Plates, PhD Thesis, Heriot–Watt University, 2000.